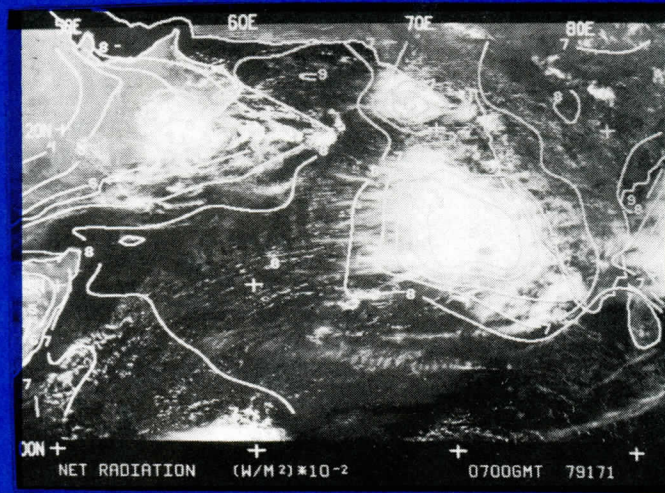


EARTH-ATMOSPHERE RADIATION BALANCE FROM GEOSTATIONARY SATELLITE DATA FOR THE SUMMER MONSOON ONSET REGION

SUMMER MONEX ONSET PERIOD: 11-20 June 1979



By

H. Virji

W. L. Smith

A. J. Schreiner

and

L. D. Herman

Space Science and
Engineering Center

NOAA/NESS
Development Laboratory

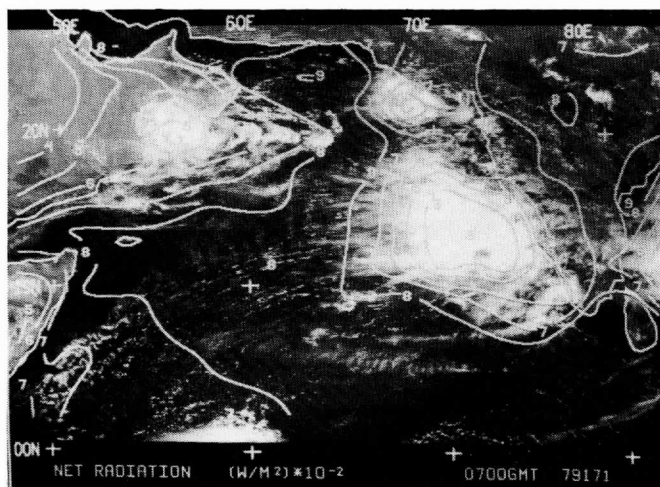
University of Wisconsin - Madison

December 1982

This page is blank

EARTH-ATMOSPHERE RADIATION BALANCE FROM GEOSTATIONARY SATELLITE DATA FOR THE SUMMER MONSOON ONSET REGION

SUMMER MONEX ONSET PERIOD: 11-20 June 1979



By

H. Virji

W. L. Smith

A. J. Schreiner

and

L. D. Herman

Space Science and
Engineering Center

NOAA/NESS
Development Laboratory

University of Wisconsin - Madison

December 1982

Table of Contents

	Page
1. Introduction	iii
2. Algorithms	iv
3. Analyzed fields	ix
4. Acknowledgments	x
5. References	xii

Hourly Fields	(Plates 1-240)
Daily Average Fields	(Plates 241-250)
Diurnal Variation at Selected Locations	(Plate 251-252)

EARTH-ATMOSPHERE RADIATION BALANCE FROM GEOSTATIONARY SATELLITE DATA
FOR THE SUMMER MONSOON ONSET REGION

1. Introduction

During the 1979 Summer Monsoon Experiment (MONEX) radiometers were flown aboard the NASA CV-990 aircraft to calibrate the narrow angle spectral-window scanning radiometer aboard the GOES-1 geosynchronous satellite stationed over the Indian Ocean. The purpose of the calibration was to enable accurate diagnoses of the detailed radiation budget characteristics throughout the life cycle of the summer monsoon circulation. GOES-1 measurements are ideal for this purpose because they possess both high spatial and high temporal resolution (1 km in the visible and 8 km in the infrared, half hourly sampling frequency). The interpretation of these data in terms of radiation budget parameters requires relationships for transforming the narrow spectral band narrow angle directional measurements of reflected and emitted radiation in the visible and infrared spectral window regions (0.5-0.9 μm and 11-12 μm , respectively) into broadband (0.2-4 μm and 4-100 μm) angularly integrated radiation fluxes of reflected solar and emitted terrestrial radiation. Such algorithms are presented in section 2. Estimates of the components of the earth-atmosphere radiation balance and top albedo obtained from application of these algorithms to the GOES-1 radiance data for the period 11-20 June 1979 form the basis of this atlas.

It is intended that this atlas be used as a reference for the evolution of the earth-atmosphere radiation balance during the onset phase of the summer monsoon. The atlas provides (a) hourly and daily averaged fields of the top radiation balance components and (b) mean diurnal variation characteristics of these parameters. GOES-1 VIS/IR imagery is also included in order to relate the evolution of the monsoon cloud cover to radiation balance. The flux data

has been interpolated, gridded and analyzed for easy inspection of the satellite derived radiation balance components. Computer tapes containing the complete data set are available from the Space Science and Engineering Center at the University of Wisconsin-Madison.

2. Algorithms

The NASA CV-990 aircraft flown during MONEX carried narrow band and broadband, narrow angle, directional radiometers (Smith et al., 1978) and broadband flux radiometers (Ackerman and Cox, 1980) to enable:

- a) The calibration of the GOES-1 0.5-0.9 μm detector digital output in terms of the reflectance of solar radiance within this spectral band.
- b) The specification of different relationships, dependent upon earth surface and cloud condition, between earth atmosphere reflectance observations in the GOES 0.5-0.9 μm region and the broadband reflectance observed over the 0.3-4 μm region.
- c) The specification of a relationship between broadband directional reflectance measured at small local zenith angles and broadband angularly integrated albedo.

The relationships provided by (a)-(c) above are used to determine instantaneous or temporally averaged albedo and absorbed solar radiation from the GOES-1 visible channel data.

The GOES-1 infrared window (11-12.5 μm) observations are calibrated in terms of total outgoing longwave radiation flux using a relationship based on simultaneous GOES-1 and TIROS-N multi-spectral (HIRS) radiometer data. The TIROS-N multi-spectral water vapor, carbon dioxide, ozone, and window radiation emission measurements over the 3.7-16 μm region were transformed into total

terrestrial flux values spectrally and angularly integrated using a relationship based upon theoretical calculations. GOES-1 IR data was not calibrated using the aircraft pyrgeometer flux measurements directly because of the problem of registering the fields of view of the narrow angle satellite radiometer and the wide angle aircraft pyrgeometer and because of the significant contribution to the total outgoing longwave flux from the upper troposphere and stratosphere above the aircraft. Intercomparison of the TIROS-N longwave flux estimates with high altitude longwave flux observations by pyrgeometers aboard the CV-990, however, compared to within 5% over a wide range of homogeneous surface conditions (i.e., cloud-free desert, cloud-free ocean, and extended cloud).

The relationships between the GOES-1 radiometer data and shortwave and longwave fluxes were obtained using data from several CV-990 flights over a variety of surface and cloud conditions (e.g., desert, vegetation, ocean, and opaque and semi-transparent cloud). Table 1 summarizes the characteristics of these flights.

TABLE 1
CHARACTERISTICS OF CV-990 FLIGHTS USED FOR CALIBRATION ANALYSIS

<u>Date</u>	<u>Flight</u>	<u>Origin</u>	<u>Objective</u>
May 14	10	Dhahran	Saudi Arabia Land/Sea Heating Differential (Albedo of Desert and Ocean)
June 5	15	Bombay	Albedo Survey of North-Central India (Albedo of Vegetated Terrain)
June 12	18	Bombay	Land/Sea Heating Differential Along N-S Meridian (75E) (Albedo of Ocean and Terrain)
June 15	20	Bombay	Monsoon Flow Pattern (Albedo of Clouds)
June 18	22	Bombay	Monsoon Flow Pattern (Albedo of Clouds)

The selection of time and space coincident aircraft, GOES-1 and TIROS-N radiation observation values was accomplished using the Man-computer Interactive Data Access System (McIDAS) developed by the University of Wisconsin (Suomi and Menzel, 1980). The GOES-1 and TIROS-N images, coincident in space and nearly at the same time as CV-990 flights, were stored in sequence in McIDAS for processing with the aircraft information. The aircraft flight track was superimposed on the images at 10 minute time intervals using the McIDAS graphics capability. Nearly colocated aircraft and satellite data were then selected manually by placing a cursor on the TV image of the satellite data at the appropriate position along the aircraft flight track. The manual selection of the space and time coincident data insured that the viewing conditions were homogeneous with the area encompassing the fields of view of the aircraft and satellite borne radiometers.

Table 2 shows the linear regression equations and their standard errors of regression used to describe the relation between the various radiometric data. It is noted that only relations (1) and (4) depend directly on the GOES-1 data. Relations (2) are achieved from the multi-spectral radiometer (MSR) 0.3-4.0 μm and 0.5-0.9 μm (matched GOES-1 filter) directional radiances observed from the CV-990 and relation (3) is obtained from CV-990 MSR 0.3-4.0 μm directional radiance observed at small view angles and simultaneous 0.3-4.0 μm flux pyronometer observations. Relation (4) is obtained from nearly colocated GOES-1 and TIROS-N infrared radiance observations.

TABLE 2
RESULTS OF REGRESSION ANALYSIS USED TO DETERMINE GOES-1
ALBEDO AND LONGWAVE FLUX CALIBRATION RELATIONS

Equation	N	RMS	CC	Condition
1: $r_g = 0.0000164C_g - 0.00077$	116	0.052	0.98	All
2: (a) $r_b = 0.749r_g + 0.01747$	65	0.003	0.99	Ocean
(b) $r_b = 0.736r_g + 0.02385$	55	0.007	0.99	Thin Cloud
(c) $r_b = 0.600r_g + 0.08849$	48	0.012	0.99	Thick Cloud
(d) $r_b = 0.840r_g + 0.03116$	32	0.007	0.99	Vegetation
(e) $r_b = 0.781r_g + 0.08399$	92	0.003	0.99	Desert
3: $A = 1.174r_b$	91	0.023	0.99	All
4: $F = 0.543\sigma T_g^4 + 44.538$	83	12 w/m ²	0.99	All

C_g \equiv the square* of the digital brightness (0-255) obtained from the GOES-1 visible channel detectors divided by the cosine of the solar zenith angle and earth-sun distance factor.

r_g \equiv reflectance for the GOES-1 spectral region (0.5-0.9 μ m) as measured from CV-990.

r_b \equiv broadband (0.3-4.0 μ m) reflectance as measured from CV-990.

A_b \equiv broadband angularly integrated albedo as measured from CV-990.

F \equiv longwave radiation flux (w/m²) as measured from TIROS-N.

T \equiv GOES-1 brightness temperature ($^{\circ}$ K).

σ_g \equiv Stefan-Boltzman constant (5.66×10^{-8} w/m²-deg⁻⁴).

N \equiv number of observations used to obtain linear fit.

RMS \equiv root mean square deviation of data from linear fit.

CC \equiv correlation coefficient.

* The digital brightness count is generated from a function of the square root of the detector output (radiance).

The relationships (1)-(3) are applied to the GOES-1 visible channel data in a step-wise fashion to estimate the shortwave flux reflected to space from the area viewed. After equation (1) is applied to the linearized GOES-1 digital data (digital count squared divided by the cosine of the solar zenith angle and the earth sun distance factor), the appropriate relation between broadband and GOES-1 narrow band reflectance is chosen on the basis of: (a) land or ocean,

(b) the GOES-1 reflectance value (the result of equation (1)), and (c) the corresponding GOES-1 infrared brightness temperature value. The thresholds used to specify the appropriate relationship are given in Table 3.

TABLE 3
CRITERIA FOR SELECTING PROPER RELATION BETWEEN BROADBAND
AND GOES-1 VISIBLE BAND REFLECTANCE

Equation	Condition	Reflectance/IR Brightness Temperature Condition	
		Land	Ocean
2(a)	Ocean		$r_g \leq 0.15$
2(b)	Thin Cloud	$0.28 < r_g \leq 0.50, T_g < 290$	$0.15 \leq r_g \leq 0.50$
2(c)	Thick Cloud	$r_g > 0.50$	$r_g > 0.50$
2(d)	Vegetation	$r_g \leq 0.28, T_g \geq 290$	
2(e)	Desert	$0.28 \leq r_g \leq 0.50, T_g \geq 290$	

The result of equation (2) is then used in (3) to obtain an estimate of the albedo, A. Subsequently the reflected solar flux is calculated using the relation

$$F_s = A I_o \mu_o d \quad (5)$$

where I_o is constant, 1375 w/m^2 (Hickey et al., 1980), d is the earth-sun distance factor (square of the ratio of the solid angle subtended by the sun at the time of the observation and the annual mean value), and μ_o is the cosine of the solar zenith angle at the location of the viewed spot. The longwave flux, F_L , is then estimated using equation (4). Spatial averages of the 8 km resolution values over $250 \times 250 \text{ km}$ areas are then calculated. For each 250 km area (approximately $2^\circ \times 2^\circ$) the absorbed solar radiation flux

$$F_A = I_o \mu_o d - F_s \quad (6)$$

and the net radiation flux,

$$F_N = F_A - F_L \quad (7)$$

are calculated. Daily average values are obtained from an integration of hourly results.

It is noted that for the region analyzed, the variability in the GOES infrared radiance observations due solely to view angle variations (i.e., limb darkening) is negligible and therefore not taken into account. Also, variations in the visible channel radiance due to the angular dependence of target reflectance is not taken into account because this variability is small compared to the reflectance variability within and among the 250 x 250 km sample regions due to cloudiness. For the Arabian Desert, which is generally devoid of cloudiness, the implicit diffuse scattering assumption is valid because of the sand surface.

3. Analyzed fields for the monsoon onset region

a. Hourly fields

All data from 26°N to Equator and 46°E to 84°E were analyzed on a 2° x 2° grid. No analysis was performed when hourly GOES-1 data was unavailable. Such instances are labelled as "NO DATA" in this atlas. The few cases when the satellite imagery was of questionable quality due to bad scan lines are labelled as "?." The times of unavailable and questionable satellite products are listed in Table 4. Out of a total of 240 time periods analyzed from 11-20 June 1979, the satellite products were missing or of questionable quality around 6% of the time.

TABLE 4
A Listing of Unavailable or Questionable
GOES-1 VIS/IR Data During the Onset Period

DATE 1979 June	HOUR (GMT)	STATUS OF GOES-1 DATA	
		VIS	IR
11	00	N	N
	01-04		N
	14-15	N	N
13	06-15		Q
	16	N	N
15	13		Q
16	10	N	N
18	11	Q	Q
19	10	Q	Q

N: No data Q: Data quality questionable

The analyzed hourly radiative flux fields for the above period are shown in Plates 1-240. These fields depict the evolution of the earth-atmosphere radiation balance components during the formation of the onset vortex of 1979 summer monsoon. The well defined hourly variability in the structure of these fields describes the diurnal modulation of the flux parameters. For five selected locations, the average diurnal variation in the top radiation balance parameters during the onset phase is shown in Plates 251-252. These locations were selected as representative of the general conditions over the Saudi Arabian desert, the clear region in north central Arabian Sea, the Indian sub-continent, the equatorial trough region, and the low level jet region off the Somali coast.

b. Daily averaged fields

The hourly flux values were integrated and analyzed to obtain the daily averaged top radiation balance components. The mean top albedo represents an integration of seven consecutive hourly top albedo values per day, centered around the local noon hour at 12°N, 65°E. In contrast, the daily average flux values represent an integration over all hours of the day. For the few cases when the hourly data was unavailable or of questionable quality, the flux

values were interpolated from the nearest available hourly data before performing the integration into daily averages. As the GOES-1 infrared radiance data for the first 5 hours of 11 June 1979 were unavailable, the daily averaged flux values for this day may not be very reliable at individual grid locations.

The daily averaged fields of the radiation balance components for the monsoon onset phase are shown in Plates 241-250. A description of the evolution of the major features of the radiation balance components based upon these fields is given in Smith et al. (1981).

4. Acknowledgments

The material contained in this atlas is part of an ongoing cooperative research program between the scientists at the NOAA/NESDIS Development Laboratory and the Space Science and Engineering Center, University of Wisconsin-Madison. The diligent efforts of the scientists of the above groups are gratefully acknowledged. Tom Rust processed photographs of GOES imagery and analyses taken on the McIDAS facility and Gail Turluck typed the manuscript. This work is funded by the National Science Foundation (NSF) under grant ATM-8205386; we gratefully acknowledge the enthusiastic support of J. Fein and P. Stephens of NSF for this work.

5. References

- Ackerman, S., and S. K. Cox, 1980: Colorado State University Radiation Instrumentation and Data Reduction Procedures for the CV-990 During Summer MONEX. Colorado State University, Atmospheric Science Paper No. 325, Fort Collins, Colorado.
- Hickey, J. R., F. House, H. Jacobowitz, R. H. Maschoff, P. Pellegrino, L. L. Stowe, and T. H. Vonder Haar, 1980: Initial Solar Irradiance Determinations from Nimbus-7 Cavity Radiometer Measurements. Science, 208, 281-283.
- Smith, W. L., D. Q. Wark, P. G. Abel, and S. K. Cox, 1978: The CV-990 Multi-spectral Scanning Radiometer (MSR) Measurement Program for the MONEX. Proposal to the National Science Foundation from the National Environmental Satellite Service (NOAA), Washington, D.C.
- Smith, W. L., L. D. Herman, T. Schreiner, H. B. Howell, and P. Menzel, 1981: Radiation budget characteristics of the onset of the summer monsoon. Proceedings of the International Conference on Early Results of FGGE and Large Scale Aspects of its Monsoon Experiments, Tallahassee, Florida.
- Suomi, V. E., and P. Menzel, 1980: The University of Wisconsin VAS Data Processing System. Report to NASA under Contract NAS5-21965 from the Space Science and Engineering Center, University of Wisconsin, Madison, Wisconsin.

